Electrostatic accelerated electrons within information horizons exert bidirectional propellant-less thrust

Becker, F. M.   Bhatt, Ankur S.

October 1, 2018

Abstract

During internal discharge (electrical breakdown or field emission transmission), thin symmetric capacitors accelerate slightly towards the anode, in contradiction to standard physics. The effect can be predicted by core concepts of a model called quantised inertia (also known as MiHsC) which assumes inertia of accelerated particles, such as electrons, is caused by Unruh radiation. This discrete Unruh radiation forms standing waves between the particle's boundaries to a Rindler horizon and a confinement horizon, which are established based on special relativity in concert with quantum mechanics. Electrons accelerate toward the anode and are assumed to encounter an inhomogenous Unruh radiation condition causing a force suggested by a modification to their inertial mass. To conserve momentum, the overall mechanical system moves in the direction of the anode. This resulting force is assumed to be caused by an energy gradient in between the confinement and the Rindler zone and its equation is derived directly from the uncertainty principle. Various thicknesses of discharging capacitors are compared to show the agreement between the experimental findings and a virtual particle oscillation associated with a standing wave energy gradient hypothesis.

Keywords: electric propulsion, Unruh radiation, Rindler Horizon, electron discharge thrust, quantum vacuum thruster, QVT, quantised inertia, imFaB, discrete virtual particle spectrum, quantum foam, information horizon energy gradient

1 Introduction

It was experimentally observed (Becker F.M. 1990) that a thinly charged parallel plate capacitor supplied with high voltage values of 5 kV DC - 10 kV DC exerted an observable force anomaly towards the anode. This anomaly only was observable with dielectrics of lower dielectric breakdown strength. Increasing the material's dielectric breakdown voltage (and thickness) resulted in the disappearance of the observed anomaly. The anomaly was disregarded as a likely artifact. A few years later, it was

speculated that electric discharge could have been the cause of the effect, but no further testing had been conducted. The observations suggested that stronger dielectrics, resulting in better performance of dielectric strength, would not lead to an effect. The electric discharge (breakdown of insulation leading to partial discharge, full discharge or field emission) would be relevant for the occurrence of the effect. Also Talley R.L. [11] had described an anomalous observation which might have been caused by accelerating electrons or electric charges. For those previous experimental observations, there was presently no explanation for this behavior in the models of standard physics, as in the present perspective would violate the concept of the conservation of momentum.

A variety of capacitive discharge experiments were conducted in 2017/2018 resulting in repeatable observations of a directional force during field emission and insulation breakdown discharge of parallel capacitive charged plates. We established experimental data demonstrating an exponential increase in the observed force when the capacitor electrode distance was decreased based on a constant amount of accelerated mass. The thrust force was observed to be linearly dependent on the accelerated mass. The effect was only observable under certain conditions with a very short capacitor plate separation distance. Additionally, the uniform discharge, the cause of the acceleration of only electrons, was essential for a valid, stable observation of the effect. If an electric discharge, such as bridging the electrodes by arcing occurred, this would introduce positive charges to the system which would hinder the effect since, as per the hypothesis, they would be accelerated in the opposite direction from the electrons. It should be noted that the force is also reversible when conductive material (but insulated from the cathode) is inserted into the zone behind the accelerated electron. This material would be located in-between the cathode and a theoretical accelerated Rindler horizon associated with the accelerated propagation of the particles employed in the discharge.

We refined a simulation of a physical model allowing the prediction of the measured force values by using aspects of the uncertainty principle and concepts derived from the theory of quantised inertia. This was done using a simple equation associated with virtual particles (photons, Unruh radiation) derived from the information boundary of a Rindler horizon and the information deflection scenario of the anode inside the electron propagation path introducing an energy gradient. In the experiment, this would have to be sufficiently high to become observable. The results are shared in this document in the method section.

2 Experiment setup and test apparatus method

2.1

As a means to provide a high acceleration to particles, electrons are relatively easy to control. Higher field strength achieved in thin electrode separation distances can provide constant electron accelerations on the magnitude of 10^{19} [m s^{-2}]. This acceleration would be associated directly to a Rindler horizon distance and with a presumed maximum wavelength [8] of the spectrum of Unruh radiation. This is done by considering only allowed radiation with nodes at the boundaries [7] which are able to be attenuated with conductive plates in the range of normal engineering practice. High field strength will liberate electrons by the field emission effect [5]. Additionally, to obtain higher force values, the application of heat [9] (Schottky effect, thermionic emission) had been seen beneficial as well.

2.2

Capacitors were designed with polyethylene dielectric materials. Other materials, such as paper, glycerin, and porous plastics, were also used but this resulted in discharges involving ionic charge flow which traveled in the opposite direction of the electron flow. Furthermore, some materials may include voids that introduce partial discharges [3] where electron avalanches generate ion current contribution inside the small void confinements. Additionally, paper insulators were ineffective to find a demonstration of a thrust effect since the atmospheric electron avalanches (Paschen law [2] for breakdown distances) would liberate secondary electrons but would also cause ionization. Overall, it is assumed that for future commercial application of a thruster device using the observed effect, a vacuum propagation of the accelerated electrons, or the application semiconductor of cathode arrays, could be the most effective method to obtain a controllable effect. Considering the available power sources (5 kV DC, 10 kV DC) the field strength would be below the actual effective tunneling field strength required to provide a sufficient reliable current density to support the effect. Therefore, the homogeneous field had to be changed into an inhomogeneous field to increase the field strength, which was done by cutting into the electrode or by using sandpaper on the cathode surface to facilitate field emission. This was done using an exacto knife applying a high number (hundreds) of small cuts or the usage of very fine sandpaper. Applying a sharp edge contributes to a higher field strength by the use of inhomogeneous electric fields, similar to the concept of a needle electrode.

For some tests, typically associated with higher thrust force values, the overall capacitor had been preheated for testing up to approximately 50 °C before placing the device onto the measurement apparatus. This also denotes that testing attempts at low ambient temperatures without pre-heating may lead to unsuccessful observations (without an observable thrust effect.)

2.3

Confirmation tests had been conducted by placing the capacitor into a sealed container with a soft vacuum. Furthermore, it was shielded by wrapping the container inside a conductive (grounded) outer layer. Such tests resulted in equivalent results as the

open air testing method. Additionally, it appears that the spread of data points have a smaller standard deviation compared to the open air method.

2.4

The supply wires had been twisted [1] to reduce electromagnetic effects (Lorentz force etc.) This was done carefully as to not influence the system and provide torque. Nevertheless, the theoretical contribution, with respect to the actual supplied current, would not contribute to an observable effect. Furthermore, to obtain a correct measurement, it had to be assured that the supply conductors were routed a sufficient distance as not to affect the load cell of the digital scale (by electromagnetic field disturbances.)

2.5

Dielectrics used did not contain a large atmospheric layer between the electrodes since the construction was tightly fit. If an air layer was present, this could lead to ions traveling in the opposite direction of the electrons due to avalanche processes by direct arcing. This would result in no directional weight modification (observed) which could present a scenario resulting in heavier weight observations only. This might also occur in certain materials when the high field strength introduces internal partial discharges in enclosed material voids where electrons as well as secondary avalanche electrons can generate positive charged ions.

2.6

It was essential to protect the measurement tools/devices of the circuit from the influences of voltage transients that could occur in a situation where the insulation resistance of the capacitor would be massively breaking down. In such cases, the shunt resistor would take over a higher voltage due to the voltage divider characteristic of the circuit since the capacitor's insulator would have a reduced resistance. The displayed circuit, as introduced in this paper, does not contain various options to apply transient surge protective devices or other preventive measures. By introducing a large resistor in series with the shunt, this could serve as a voltage divider in the case of insulation failure. Such transient effects are seen more likely when the field emission current is increasing. Also heating of dielectric insulation material could reduce the insulation resistance of the dielectrics.

2.7

An alternative to the 5 kV DC commercial power source was also used. A flyback transformer with a maximum output slightly above 10 kV DC has been utilized for voltage sweeping on experiments to vary the electron's acceleration (property of the Rindler horizon.) The flyback transformer was supplied in the primary winding by a conventional DC power supply. The output voltage characteristic had been interpolated by the data specifications of the flyback manufacturer and was rectified (smoothed) by the tank capacitor.
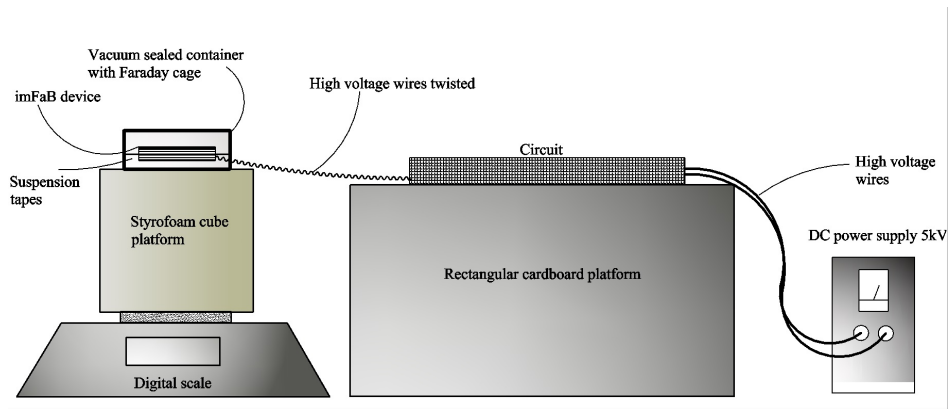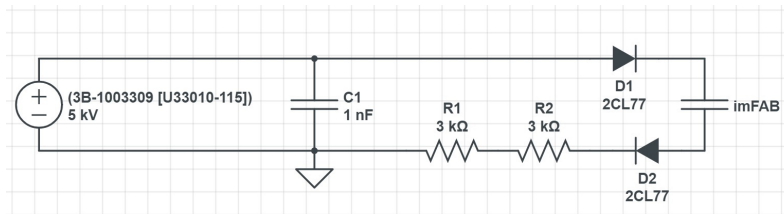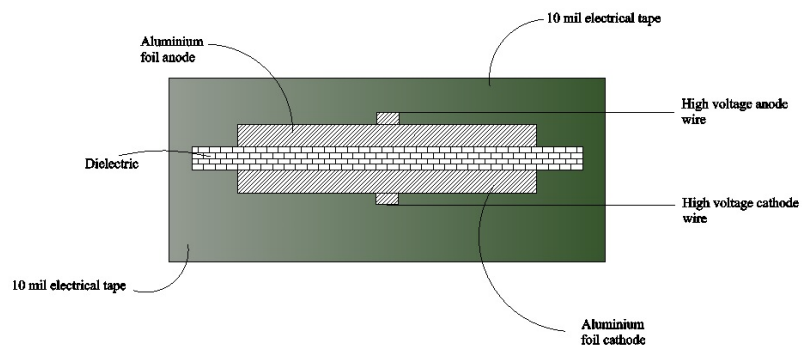
Figure 1: Experiment setup

Figure 2: Functional circuit

Figure 3: General prototype construction

3 Experiment observations

3.1 Thrust observation versus electrode distances

The electrode distance had been varied and the force had been monitored. Also, since the discharge current is dependent on the Schottky effect (field enhanced thermionic emission), which not only considers the electric field strength but also the heat of the surface, the actual current for each data point would statistically fluctuate. Therefore, the graphs illustrating the results of the current measurements are normalized to a constant value (same charge amount, same accelerated mass.) These explained predictions also correlate to a proposed hypothetical model of a quantum oscillator which provide a discrete spectrum where, within this document, Unruh radiation is generated by a Rindler horizon information boundary by acceleration.

If a constant current (accelerated mass) was provided, the shortening of the electrode distance (the thickness of the capacitor's insulation layer) would cause the thrust force effect to exponentially increase in value. The electrode distance, or insulation thickness, is referred throughout this document as equivalent to the confinement distance or horizon distance (see graphs). Those descriptions should be seen as equivalent for this research.

The result of the first sub-experiment focused on accelerated electrons with different insulator thicknesses, between 13 μm to 80 μm, influencing the acceleration voltage and the information horizon boundaries. A total of 266 data points were collected. Here, the measured current value was standardized (as fluctuating under the effect of field emission) to a normalized current level of an arbitrary 10 μA. The accelerated voltage was selected as 5 kV for all measurement points throughout the capacitors with different insulation thicknesses. The acceleration voltage of approximately 5 kV corresponds to an electric acceleration of around 10^{18} to 10^{19} [m/s^2] for the various electrode distances used in the experiment.
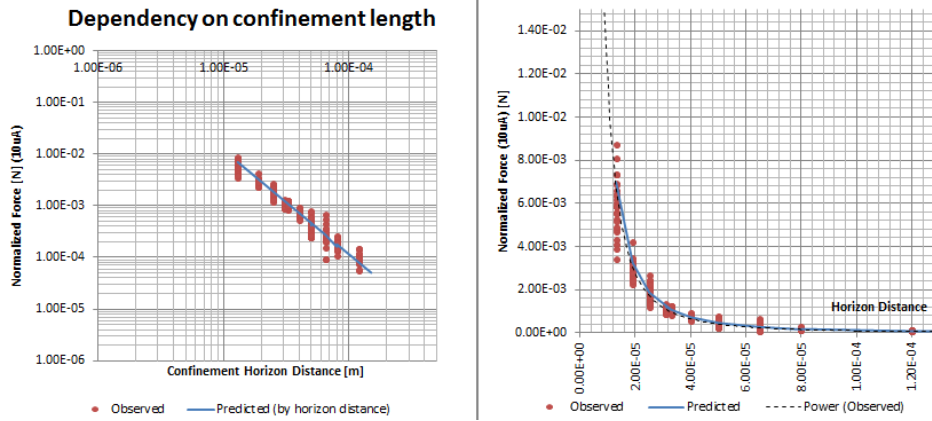

Figure 4: Normalized force versus distance

We observed that a force modification when altering the electrode distance follows a linear trend in a logarithmic view. Hence the trend is attributed to an exponential increase of force by a linear reduction of the electrode distances. Later, this will be defined as a horizon distance or confinement of the seeing zone (an expression by Mc-Culloch, the propagation direction) which is in front of the accelerating particle.

If not indicated, data points of individual graphs are considered an absolute value hence, these points include both directional scenarios. The anode of the capacitor pointing upwards was associated to an upward acceleration while the anode pointing downwards was associated with a downward acceleration. This always held true as long as no reversal force mechanism (see section 3.3) was introduced which will be discussed later.

In Fig. 5 the actual force direction shows dependency on the accelerated mass measured with the proportional electric current. The symmetry of the data points illustrates that the observed force appears independent of influences of gravity, ionic winds, thermal buoyancy and other such artifacts. Finally, the tests, which had been conducted within a sealed and air pressure reduced containment (low vacuum) identified as 'vac' in the attached graph, follow the trend line more closely compared to the open air measurement points.
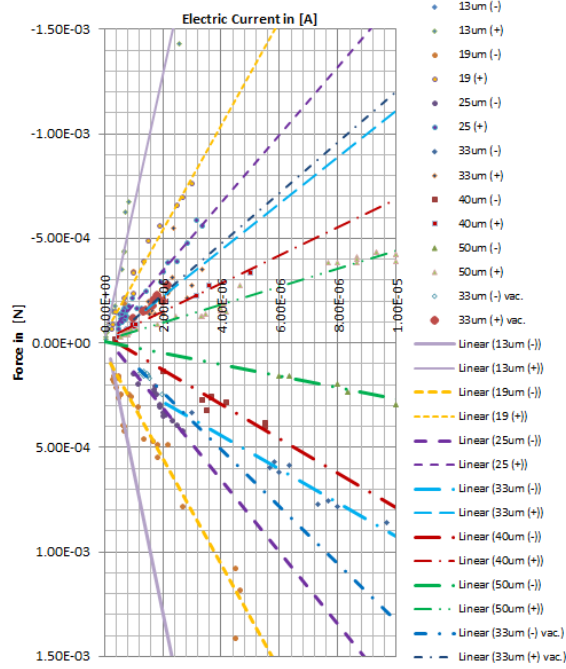

Figure 5: Force versus Current

The operational characteristic of the identified thrust effect correlates to a linear dependency on the amount of accelerated mass and is exponential per higher force gradient with decreasing electrode (confinement) distance.

Note: Also the graph shows, for thicker insulators, the observed thrust was greater when the anode (+) was oriented on the top of the capacitor. This fact could be correlated to a slight influence of buoyancy, since, in order to obtain higher observational values, the devices had been preheated.

As advised by Prof. Dr. M. Tajmar (University Dresden, pers. comm.) the effect had also been tested by measuring the force of the capacitor plates in a vertical position which resulted in a positive "null test". This critical plausibility examination resulted in no force while in vertical position. Henceforth, the device and thrust force passed the plausibility criteria.

Another graph with a different view on the operational characteristics shows similar trend lines compared to the utilized estimated power consumption.
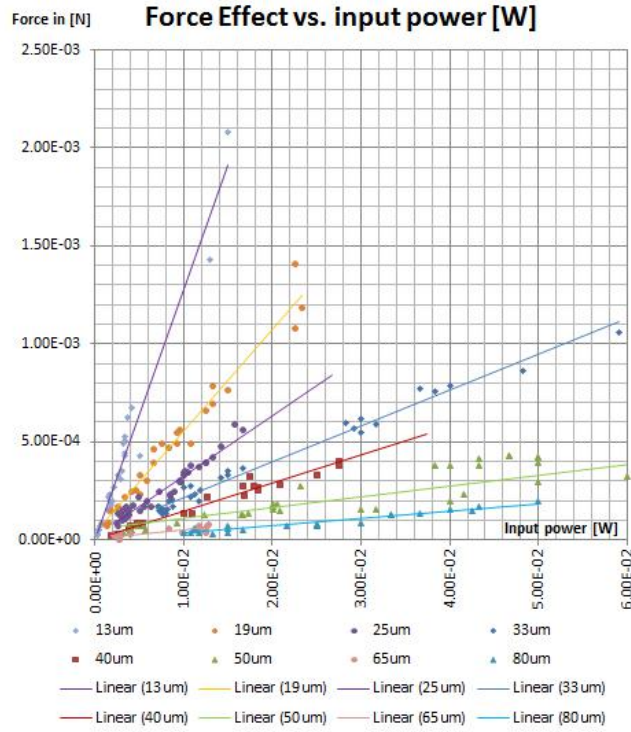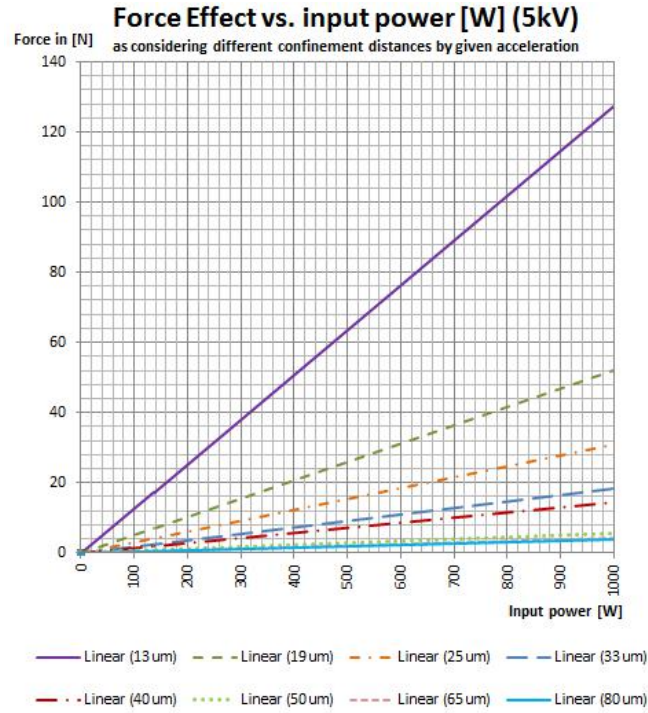

Figure 6: Force versus input power

Figure 7: Force versus input power extrapolated

The same graph can be extrapolated to show the force versus power ratio of a scaled up thruster device up to 1 kW input power.

Furthermore, the effect and operational thrust characteristics can be displayed by combining the square root of the accelerated mass and the energy gradient between the Unruh baths into one factor. The linearity in the logarithmic scale shows the combined dependency of the elements of the mass and Unruh radiation energy related to the accelerating particle.

Note: This view provides the advantage to compare all electrode separation distances in one combined graph.
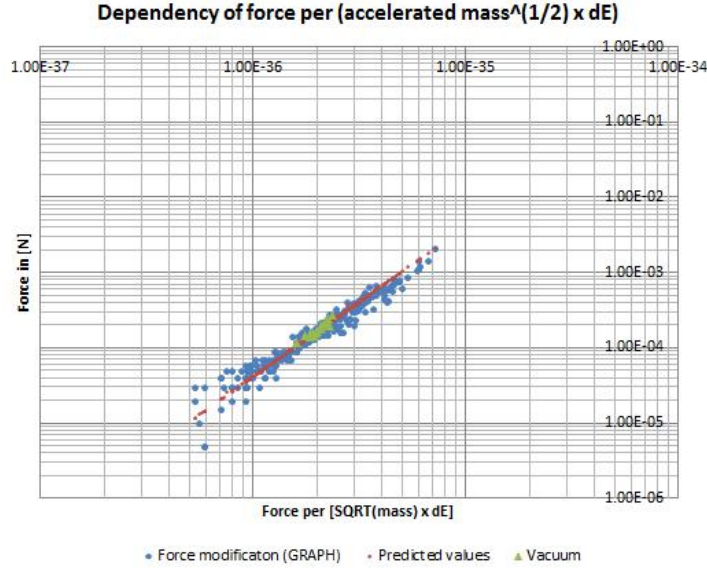
Figure 8: Force versus accelerated mass and energy

The use of the low vacuum container, where the thrust device is placed and shielded inside, appears to stabilize the measured data points versus prediction.

3.2 Thrust versus change of acceleration voltage as proportional to the Rindler distance

The Rindler distance is determined by the electric field strength and acceleration. Electric acceleration is yielded by the following: electric field strength multiplied by the elementary charge divided by electron mass $a_e = Eq/m_e$. Here the electric field strength is determined by voltage divided by electrode distances. In reference to the works of M.E. McCulloch, the Rindler distance had been calculated by the square of the speed of light divided by the acceleration $R = c^2/a$ [6].
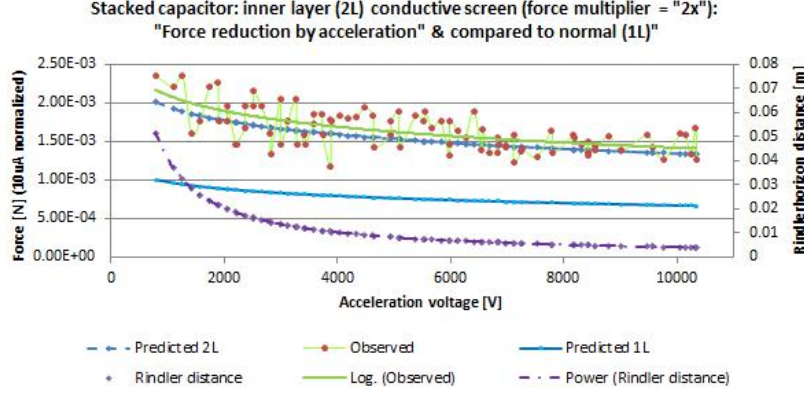
Figure 9: Force versus acceleration voltage for double layer capacitor

As increased voltage was applied, a slight decrease in normalized force occurred. Voltage was swept from 1 kV to approximately 10 kV and a total of 97 data points were collected. Furthermore, another effect was observed by stacking capacitor elements in series to provide a force multiplier condition. In regards to the reduction of the effect force with an increase in voltage, this showed an interesting operational characteristic. This characteristic implied an increase of the effect corresponded to the reciprocal of the kinetic energy of the accelerated electrons (with increasing kinetic energy of the particles the effect is reduced.)

With respect to the force multiplication for these measurements, a normal capacitor had not been used but rather a modified one, which had incorporated an additional inner conductive floating material similar to the cathode/anode foil between the two insulators. Such an arrangement represents a series capacitor which meant that the voltage was divided by approximately half. Assuming that the supply current outputted the same volume of electrons, the results suggest that the particle mass got accelerated twice. The prediction method, (see section 4) using the amount of events for each accelerated particle, would only yield about half of the measured force value. Doubling the amount of events, since the electron gets re-accelerated from the inner floating plate, resulted in a prediction that would be in compliance with the observation.

It should be noted that by using the proposed physical model, a reduction of the Rindler distance compared to the confinement zone (located in front of the accelerating particle), would reduce the number of unshared wavelengths hence, would influence the energy gradient. This influence resulted in a decrease in dE, which was the energy difference between the potentials of Rindler zone and propagation area.
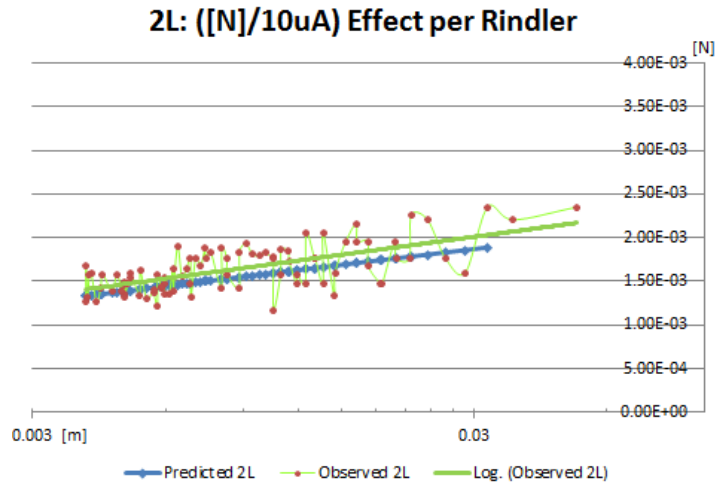
11

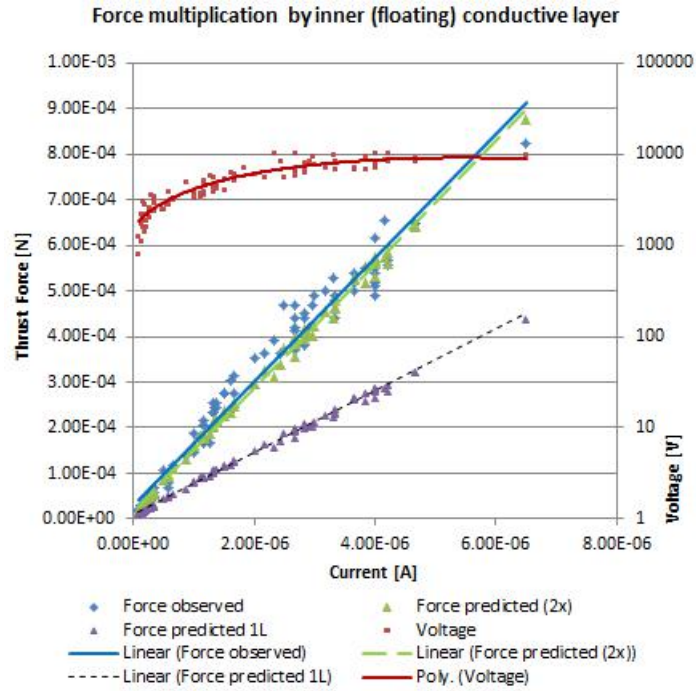Figure 10: Force versus Rindler distance at $10\mu A$

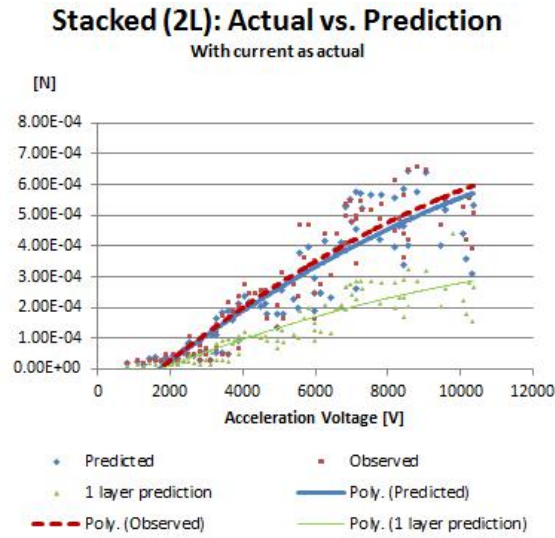Figure 11: Force versus current for double layer capacitor

Figure 12: Force versus voltage for double layer capacitor

For reference Fig. 13 illustrates the overall weight modification which was observed during the various experiments.

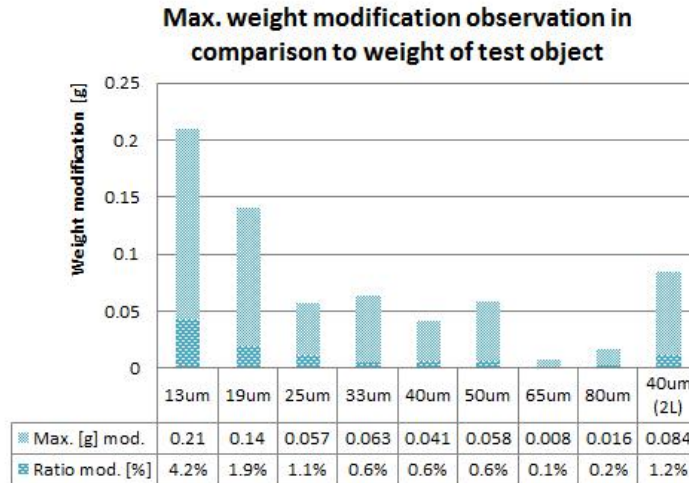|	13um	19um	25um	33um	40um	50um	65um	80um	40um (2L)
Max. [g] mod.	0.21	0.14	0.057	0.063	0.041	0.058	0.008	0.016	0.084
Ratio mod. [%]	4.2%	1.9%	1.1%	0.6%	0.6%	0.6%	0.1%	0.2%	1.2%

Figure 13: Maximum weight modification for all capacitors

It should be noted that some capacitors showed a lower performance in the number of accelerated particles (measured electric current.) This chart is not associated to a general performance, but rather illustrates the maximum achieved amount of modification with respect to the force attraction of earth's gravity field.

3.3 Altering Rindler zone with insertion of conductive attenuation materials

Additional tests performed (144 data points) resulted in the identification of a reversal in directional force. When a particle or object is accelerated, a Rindler horizon forms behind it. Therefore, assuming the existence of this information boundary zone, an experiment had been conducted by inserting a conductive material into the zone. According to the skin depth's equation (see Appendix B), it is assumed that even a thin material could attenuate up to the maximum wavelength of the standing waves with nodes at the horizon as would be allowed by the Rindler distance.

Two different behaviors had been identified. When the thickness to the cathode is extended into the Rindler zone, the thrust effect was linearly reduced with proportion to the covered/blocked length of the Rindler zone. However, when a conductive material that was electrically insulated from the cathode had been inserted into the area at any position, a full force reversal was observed.

This suggested that the conventional acceleration changed from propagating the system from the anode direction to the cathode direction using an insulated attenuation blocker. The system provided a reversed-direction propagation towards the Rindler horizon. Furthermore, a conductive cathode connected with 100% blocking of the Rindler zone, lead to a full force reversal. Additionally, if an attenuation material was inserted in a position slightly beyond the Rindler horizon distance, (out of the causal experience of the accelerating particle), the force situation appears normal towards the anode.
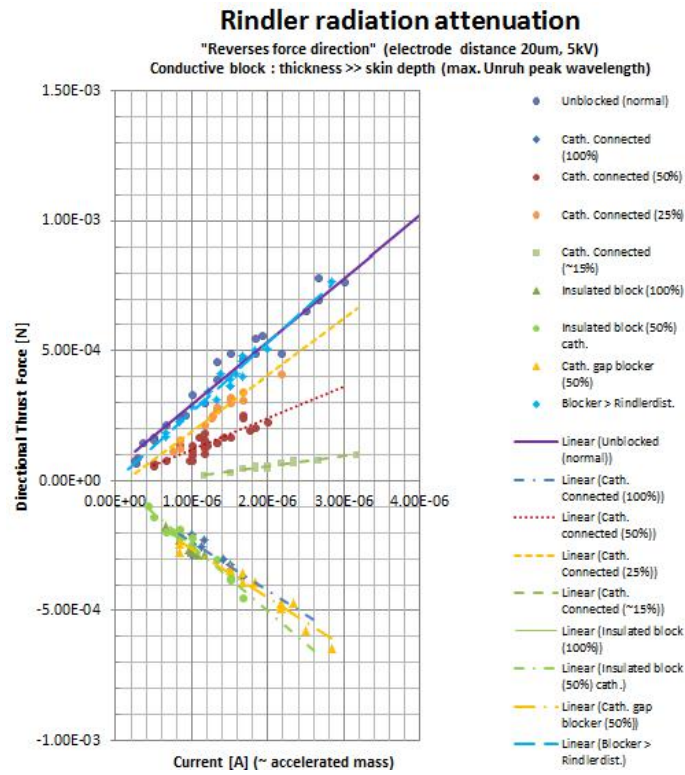
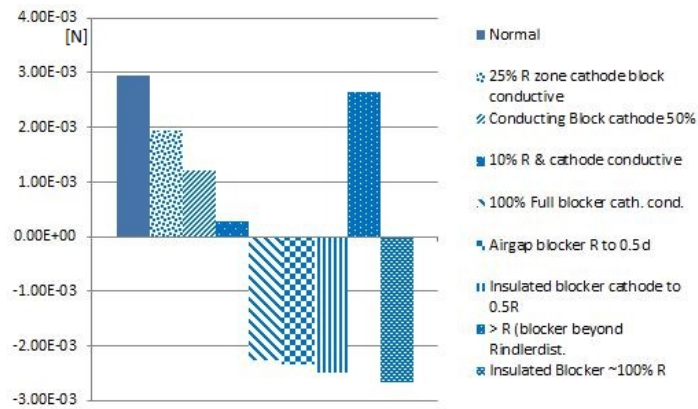Figure 14: Force [N] versus current for various blockers

Figure 15: Force [N] for different blockers

15

The observation of reversing the accelerated direction, with same level of the original thrust force, might be seen as an effect involving an accelerated frame of reference. During the original effect, the Rindler horizon propagated together with the electrically accelerated electron (co-moving) and the Rindler horizon moved as the electron traveled. Looking into this scenario we may consider this as one accelerated inertial reference frame, which is initially accelerated on the level of the electric acceleration. Physical standard models describe this (accelerated) situation by introducing one fictitious/pseudo force (adding on the electrical acceleration force vector) which denotes an additional thrust acceleration vector. As per Newton's third law, forces only exist in pairs and this inertial force on the electron's co-moving inertial accelerated frame could be assumed to be directed opposite to the accelerated direction of electron propagation. In the frame of the external observer, this fictitious/pseudo force could change the acceleration direction since the actual effect force is cancelled by the causal blocking of the Rindler horizon. In this model the other pair component of the cancelled pseudo force would remain valid and directs the acceleration direction leading to a reversal. This might happen because the energy of Rindler zone could be assumed to stay present/valid, but is not able to propagate to provide an accelerative force; hence, the inertial force pair stays in existence.
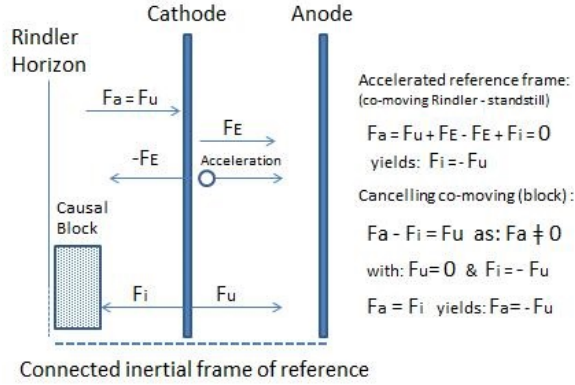

Figure 16: Inertial frame force

4   Method

In particular the fast/frequent burst electric discharge thrust effect (named FBeDT) is not only associated to capacitors, where the thrust towards the anode is caused by effects assumed from the high voltage supply [10], but is a more general effect that uses capacitors as an experimental mechanism to accelerate particles (with a defined accelerated condition). The electric acceleration is used to observe an effect caused by propagating electric charges (particularly electrons discharging in insulation breakdown and field emission tunneling into solid materials) in very high electric field strengths resulting in hyper-accelerating electrons. It also should be noted that the thrust effect (in the propagation direction of the accelerating particle) is reversible not only by changing polarity (per reversing the acceleration direction), but by altering

conditions in the space behind the accelerated electrons, namely, between the Rindler horizon and the cathode. The capacitors (in general breakdown or field emission mode) are used as a mechanism to accelerate particles with known particle mass and can be achieved within very short electrode distances.
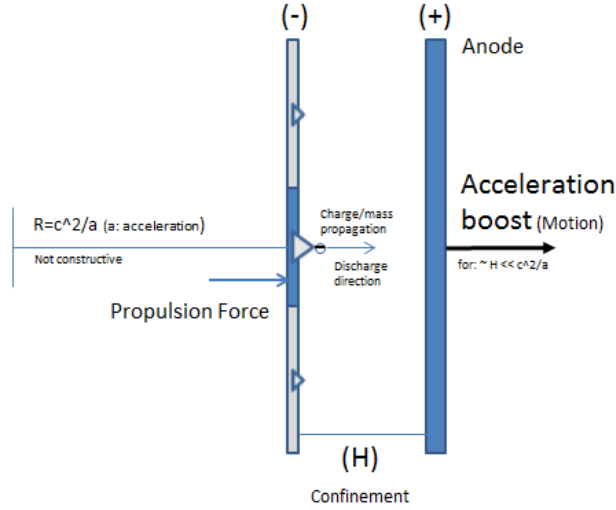

Figure 17: Force diagram of thruster

According to the latest understandings in physics it is considered probable that not only singularity horizons [4] but also Rindler horizons generate thermal radiation [12] [13]. Recent developments in theoretical physics [7] [8] assume such radiation as confined in boundaries would exist quantised with wave nodes at the horizons. Under normal conditions an accelerated particle experiences a maximum thermal Unruh radiation (peak wavelength) of approximately 8 times the maximum wavelength as confined in the Rindler horizon zone. This situation causes inertia [7] [8].

In order to alter the inertia of an object, we assume it would be possible to reduce the maximum Unruh wavelength, or equivalent associated harmonic oscillations by virtual particles. This could be established by information loss at a horizon in the region, in front (propagation direction) of an accelerating object, and therefore, reduces the (discrete, due to nodes at the horizon) spectrum and the total amount of waves allowed in the confinement. Wave attenuation, into a confinement condition, would be accomplished by reducing the distance to the information boundary and would limit the maximum radiation wavelength in front of the accelerated object and the Rindler horizon. If a confinement in the electron propagation path is established with the same distance as the Rindler horizon, an inertia equilibrium situation would be achieved. If the attenuation position is further reduced, more Unruh waves in the propagation zone would be cancelled and the total wave energy (in the zero point field) in front of the accelerating particle would be less available in the Rindler horizon zone. In the case of small particles, this would allow a one dimensional methodology to simulate the conditions.

4.1 Theoretical force model by uncertainty principle

Having documented and demonstrated that an effect exists to generate an anomalous force, the question remains whether this could also work in theory. We begin by using the uncertainty principle $\Delta x \Delta p = \hbar/2$ and the assumption that by nodes at the horizons the energy level is fully determined so the Δx would be equivalent to the maximum possible uncertainty in the given boundaries (horizons.) In this specific case, there are no rotations/orbits therefore, one will not need to use $\hbar$ and instead h will be used since electrons are traveling in a straight path (linear momentum.) Assuming that in a confined space $\Delta x \Delta p = h$ the confined attenuated energy is ΔE, this would result in the summation of the total number of virtual particle oscillation energies down to the Planck length (l_p). As the linear momentum (Δp) is equivalent (and determined) as $\Delta E = \Delta pc$.

Use the energy formula for a photon $\Delta E = \Delta pc$ and substitute in for $\Delta p = h/\Delta x$.

$$\Delta E = \frac{hc}{\Delta x} \tag{1}$$

Plug in for $\Delta x = kl_p$ in order to count all the waves in the confinement region up to N. Here l_p is denoted as Planck length. Additionally, N represents the number of the fundamental oscillations allowed in the confinement.

$$\sum_{k=1}^{N} \Delta E_d = \frac{hc}{l_p} + \frac{hc}{2l_p} + \cdots + \frac{hc}{Nl_p} \tag{2}$$

Plug in for $\Delta x = kl_p$ in order to count all the waves in the Rindler region distance (R) up to M.

$$\sum_{k=1}^{M} \Delta E_R = \frac{hc}{l_p} + \frac{hc}{2l_p} + \cdots + \frac{hc}{Ml_p} \tag{3}$$

Now compute the ratio of fractional energy that will be pushing the capacitor. Namely, the ratio $\frac{\Delta E_R - \Delta E_d}{E_R}$.

$$\frac{\Delta E_R - \Delta E_d}{\Delta E_R} = \left(\frac{(\frac{hc}{l_p} + \frac{hc}{2l_p} + \cdots + \frac{hc}{Ml_p}) - (\frac{hc}{l_p} + \frac{hc}{2l_p} + \cdots + \frac{hc}{Nl_p})}{\frac{hc}{l_p} + \frac{hc}{2l_p} + \cdots + \frac{hc}{Ml_p}}\right) \tag{4}$$

Now write the equation in closed form and simplify.

$$\frac{\Delta E_R - \Delta E_d}{\Delta E_R} = \frac{\sum_{k=1}^{M} \frac{1}{k} - \sum_{k=1}^{N} \frac{1}{k}}{\sum_{k=1}^{M} \frac{1}{k}} \tag{5}$$

Now, replace M with the total waves in the region $R/l_p - 1$ which are the total waves in the Rindler region down to Planck length. Also replace N with $d/l_p - 1$ which are the total waves in the confinement region. Finally, multiply by hc/d using (1) to get the total energy gradient of one electron.

$$\Delta E_e = \frac{hc}{d} \frac{\sum_{k=1}^{R/l_p - 1} \frac{1}{k} - \sum_{k=1}^{d/l_p - 1} \frac{1}{k}}{\sum_{k=1}^{R/l_p - 1} \frac{1}{k}} \tag{6}$$

18

Use the closed form approximation for a harmonic series formula namely, $\sum_{k=1}^{N} \frac{1}{k} \approx ln\frac{2N+1}{2(1)-1}$ for both summations. This yields the same results as applying the Euler-Maclaurin formula for harmonic series, namely $\sum_{k=1}^{k} ln(k) + \gamma + \epsilon_k$ where γ is Euler's constant and ϵ_k represents the higher order error terms.

$$\Delta E_e \approx \frac{hc}{d} \frac{ln(\frac{2R}{l_p}) - ln(\frac{2d}{l_p})}{ln(\frac{2R}{l_p})} \tag{7}$$

Fig. 18 suggests that a correlation with the physical action exists. The area under the curve represents [J m] which is the units of energy distance or action which is [kg m^{2}s].
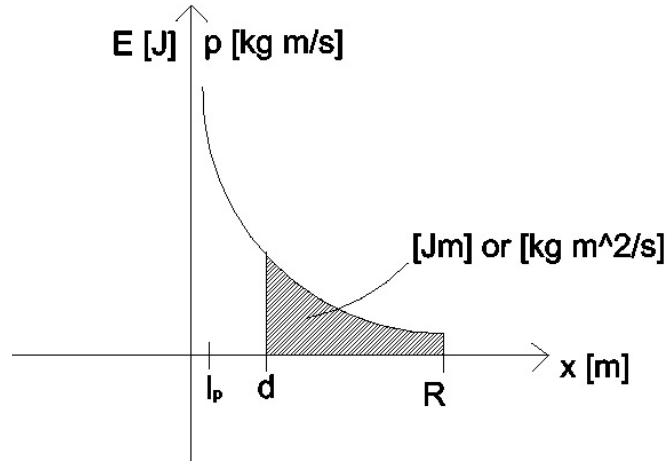

Figure 18: Energy and momentum versus distance

Note: Regarding Fig. 18 by conjugate variables, the linear momentum is the overall derivative of the corresponding action with respect to the position. In particular the uncertainty in position (also per quantum hydrodynamics) states that the action is the conjugate variable of the probability density.

Now also notice (7) can be written as the subtraction of two energy regions.

$$\Delta E_e \approx \frac{hc}{d}(1 - \frac{ln(\frac{2d}{l_p})}{ln(\frac{2R}{l_p})}) \tag{8}$$

Use the change of base formula to obtain the following. Here we have the subtraction of two energy regions. Notice the full Rindler region is not used for Δx.

$$\Delta E_e \approx \frac{hc}{d}(1 - log_{R/l_P} d/l_p) \tag{9}$$

19

Now we proceed back from (7) and combine the numerator using property of $lna - lnb = ln(a/b)$ for a more simplistic form.

$$\Delta E_e \approx \frac{hc}{d} \frac{ln(\frac{R}{d})}{ln(\frac{2R}{l_p})} \tag{10}$$

Now solve for the force $\Delta F_e = \frac{\Delta E_e}{0.5d}$ by substituting in (8). Notice the distance is to the middle of the confinement. This gradient was identified to be possible by measurement. This gradient might also denote a relation to the superimposed wave functions in a scenario where the average position of the Unruh radiation photons are in the middle of the confinement by Maupertuis's principle. Basically, the momentum of each harmonic oscillation is defined by its node from the information boundary (photons acting similar to an electron in a box scenario.) The energy eigenstate has a symmetric probability amplitude therefore, this result leads to the notion that the uncertainty in position is distributed within the zone evenly and henceforth the average position is in the middle of the confinement. On the other hand, looking into a probabilistic density of the particles over the length of the confinement, we also see that an average low density level (like an energy divergence drain) would be statistically in the middle of a confinement. This might denote that the gradient, as identified, is a probabilistic time averaged parameter.
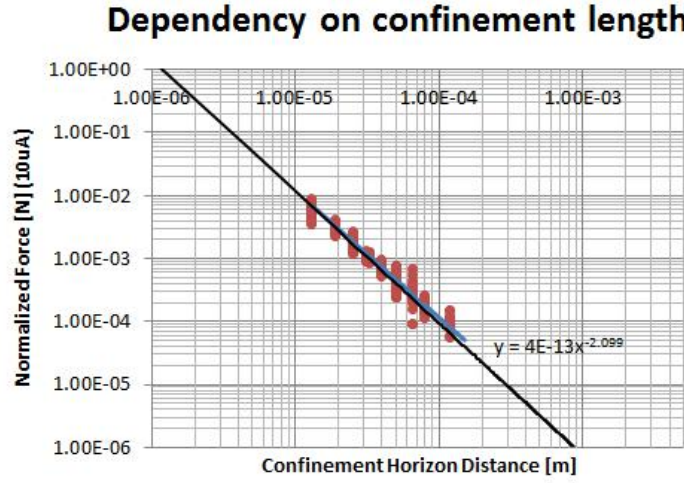

Figure 19: Normalized force versus confinement length

$$\Delta F_e \approx \frac{2hc}{d^2} \frac{ln(\frac{R}{d})}{ln(\frac{2R}{l_p})} \tag{11}$$

Finally divide the force equation by the diffraction index since the speed is reduced to c/n where $n = \sqrt{\epsilon}$ which is the diffraction index of low-density polyethylene (LDPE) plastic or mylar. We can also drop the approximation for simplicity.

$$\Delta F_e = \frac{2hc}{\sqrt{\epsilon}d^2} \frac{ln(\frac{R}{d})}{ln(\frac{2R}{l_p})} \tag{12}$$

The above results in the theoretical model for the force seen on one electron accelerated mass. Finally multiply by the number of electrons N_e to find the total force on the capacitor.

$$\Delta F = \frac{2hcN_e}{\sqrt{\epsilon}d^2} \frac{ln(\frac{R}{d})}{ln(\frac{2R}{l_p})} \tag{13}$$

4.2 Theoretical force model by Wave energy formula

One can also derive the theoretical model of the force by using the wave energy formula.

$$E = \frac{hc}{\lambda} \tag{14}$$

Now let us find the total wave energy in the confinement region letting $\lambda = 2kl_p$ to count all the waves up to N. Here the $2l_p$ comes from the fundamental wavelength.

$$\sum_{k=1}^{N} \Delta E_d = \frac{hc}{2l_p} + \frac{hc}{4l_p} + \cdots + \frac{hc}{2Nl_p} \tag{15}$$

Plug in for $\lambda = 2kl_p$ in order to count all the waves in the Rindler region up to M.

$$\sum_{k=1}^{M} \Delta E_R = \frac{hc}{2l_p} + \frac{hc}{4l_p} + \cdots + \frac{hc}{2Ml_p} \tag{16}$$

Now compute the ratio of fractional energy that will be pushing the capacitor. Namely, the ratio $\frac{\Delta E_R - \Delta E_d}{\Delta E_R}$.

$$\frac{\Delta E_R - \Delta E_d}{\Delta E_R} = \left(\frac{(\frac{hc}{2l_p} + \frac{hc}{4l_p} + \cdots + \frac{hc}{2Ml_p}) - (\frac{hc}{2l_p} + \frac{hc}{4l_p} + \cdots + \frac{hc}{2Nl_p})}{\frac{hc}{2l_p} + \frac{hc}{4l_p} + \cdots + \frac{hc}{2Ml_p}} \right) \tag{17}$$

Now write the equation in closed form and simplify. Notice the 2 that is in the denominator of each sum will factor out and cancel and will be the same result as (5).

$$\frac{\Delta E_R - \Delta E_d}{\Delta E_R} = \frac{\sum_{k=1}^{M} \frac{1}{k} - \sum_{k=1}^{N} \frac{1}{k}}{\sum_{k=1}^{M} \frac{1}{k}} \tag{18}$$

Follow the steps in previous derivation to finally result in the following.

$$\Delta F = \frac{2hcN_e}{\sqrt{\epsilon}d^2} \frac{ln(\frac{R}{d})}{ln(\frac{2R}{l_p})} \tag{19}$$

In general, the overall force will be established by multiplying the force of a single acceleration event with the number of particles (electrons) involved over the duration of one second as determined by the electric current flow (total burst amount of accelerated particles.) For the stacked capacitor, the overall force corresponds to the multiplication of the number of particles times the number of acceleration stages. Essentially, this is the force times the overall number of accelerated events within one second.

5 Discussion

The present results, due to the clear operational characteristics of the trend lines and 507 data points collected, allow for the positive identification of a new effect. The prototype thruster concepts can be modeled with an equation based on some concepts as outlined by theory of quantised inertia [7] [8] using (discrete) Unruh waves with nodes at the horizon. Since the predictive model and the experimental results are very closely converging, and no other models exist explaining the effect without violating the present law of physics, the result may also denote that an Unruh-like radiation exists. From all three sub-experiments, it is proposed that confined Unruh radiation is composed of a discrete spectrum. This particular confinement scenario and the causal information confinement by a Rindler horizon can be used for practical applications. This experiment may also suggest that it was reasonably demonstrated to assume that a Rindler horizon is a physical information boundary which emits radiation. This may provide the basis to further conclude the actual existence of an Unruh-like radiation condition. Furthermore, as the identified thrust force acts in the general inertial framework, this experiment may provide the basis of certain aspects of the theory of quantised inertia. It is suggested that tests are repeated with use of a more precise testing facility and calibrated equipment.

With regards to the topic of a discrete Unruh radiation in the confinement by the anode, it could be speculated that this is caused by the end of the field lines on an electrical horizon. For example, the accelerated electrons have their own wavelength for which the thickness of the anode material would disallow the penetration. Therefore this limits the possible interaction of the electrons and their forward path world line and they would experience full attenuation as seen in particle/wave duality. Furthermore, Unruh radiation photons, which are experienced by the electrons, would not be able to penetrate through the anode plate thickness so the Unruh waves, which are able to propagate in the seeing zone, would be virtual particles created at the location of the anode. This also suggests that the anode may operate for the accelerated electrons as a causal event horizon equivalent. The results of this experiment suggest further research on this mechanism is recommended, namely, inspecting the physical feature of the anode which could act as an information horizon which appears to be observable.

With regards to the prototype (quantum vacuum thruster), it is possible to demonstrate a modular system which is scalable and uses relatively low power consumption. These simple prototypes had a performance above $0.4N/kW$ which NASA's Dr. H. White stated as a requirement to provide a means to a crewed mission to Titan/Enceladus [14]. Construction of modular segments could also provide the advantage of being shut down individually in case of failure/malfunction without affecting the overall performance of the modular architecture of a thruster system. Since the

thruster concept is solely electric, the experimental discovery could provide first means for interstellar space exploration (see performance chart Fig. 7.)

6 Conclusion

By conducting tests on capacitive systems, which accelerate electrons within a narrow causal information horizon boundary, a force has been identified which accelerates the overall system. This thrust force is linear with respect to the amount of accelerated matter. The force occurs when the causal propagation zone is confined to less than 50% of the acceleration associated with the Rindler horizon distance. The force is directed in the propagation direction, but can be reversed by attenuating the associated horizon boundary (Unruh) radiations within the Rindler zone.

The indirect discovery of the existence of Unruh radiation (or some other oscillatory nodal waves with information boundaries within the zero point field of virtual particles) demonstrates a net force in accordance to a physical model aligned with core concepts initially outlined by McCulloch's theory of quantised inertia. The experiment has shown that a Rindler horizon physically exists and this horizon radiation provides a means to modify accelerated conditions.

A concept for an inertia modified frequent accelerated burst (imFaB) thruster has been found which is possible to scale up to commercialize and provide a new means of propellant-free electric supplied propulsion. Current values already support feasible space travel. Extrapolation of force values show that escaping gravity is possible as well.

7 Acknowledgments

8 Appendix A

Here we inspect the seeing zone conditions where the more precise seeing zone length is (with $\beta = 0.2014$ pers. comm. McCulloch) and $4\beta\pi^2 = 7.951$. For simplification we consider the maximum wavelength as suggested by McCulloch as approximately 8 Rindler distances. Basically 7 more oscillations compared to the fundamental wavelength of the Rindler zone are allowed inside the propagation path. Using (1) this results in the approximated unshared wave energy level simplified to:

$$\sum_{k=1}^{8-1} \frac{k}{8R} hc \tag{20}$$

Here, R is the Rindler distance. From computing the sum, this yields an approximate constant factor of $6.925 * 10^{-25}$ [J m] which can be multiplied with $1/R$ to determine the delta energy of the un-attenuated accelerated inertial condition (by considering the contribution of the unshared waves.) Let us call this parameter, since it is relevant for a 1 meter definition for the time being, the inertial energy factor due to the dimensional unit of [J m].

The quantised seeing zone energy of the unshared oscillations would require the equilibrium to cross the abscissa x-axis at one Rindler distance. Furthermore, in the un-attenuated confined state, the energy level at $8R$ should be the same as computed by the inertial energy factor for the inertial undamped state. In this case, the number of allowed unshared waves is 7 which is used for the total summation function.

For curve fitting, the following equation can be created to match the seeing zone equation for a general $x = R$ situation to find the constant 7.111 by adjusting the output value to the same value as the 'inertial energy' factor for 1 meter. Basically, this is accomplished by setting the confinement length to $d = 8$ Rindler lengths.

$$\Delta E = \sum_{k=1}^{7} (\frac{8-1}{8^2}) \frac{7.111k}{8} hc = 6.925 * 10^{-25} \tag{21}$$

The numerical determination of the seeing zone energy factor will be 7.111/8. Below the number of unshared waves can be computed by a integer variable that is dependent on the ratio d/R.

$$\Delta N = \lceil 7.5 - (\frac{7}{1} - \frac{d}{R}) \rceil \tag{22}$$

Now one can replace the value 8 in (23) with a more general confinement position d to find energy behavior over the change in the confinement distance while still keeping the previous numerical; estimated seeing zone related energy factor of 1/1.125.

$$\Delta E = \sum_{k=1}^{\Delta N} (\frac{d-R}{d^2})(\frac{7.111k}{8R}) hc \tag{23}$$

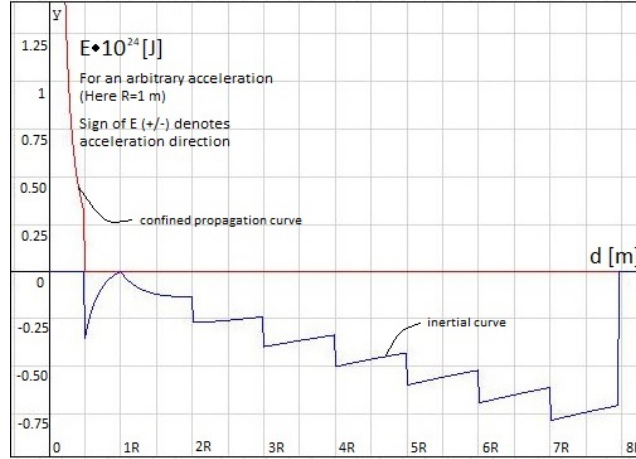The overall situation can be represented by the following.

Figure 20: Approximation of energy delta profile in confined seeing zone

By the engineering approach of curve fitting between the 2 extrema of the zero cross equilibrium at $1R$ and the un-attenuated original inertia situation energy level at approximately $8R$, it appears that the identified fitting parameter of $7.111/8$ would refer to the factor $1/1.125$ which corresponds to the increase in the original wave energy of the individual steps up to the point where the one wavelength is cancelled out (by reduction of confinement distance.) Notice the overall curve is valid for a confinement $d > 0.5R$.

In Fig. 20 at a given Rindler length inside the propagation path, a confinement situation is established which reduces the quantised wavelength in front of an accelerated particle.

An interesting note is that between $0.5R$ and $1R$ the absolute energy delta is further increasing with the further reduction of confinement length. This correlates to the situation where the energy in the Rindler zone is constant and the same wave number in the propagation path exists, but due to shorter confinements, a slightly shorter wavelength (as limited by the maximum allowed fundamental wavelength and the compulsory nodes at the boundaries) provides a higher energy level in the confinement zone. This continues until a confinement position of 0.5 Rindler length, where the fundamental wavelength is cancelled.

Fig. 20 does not include the consideration that all wavelengths in the confinement are shorter, with regards to the respective count compared to all allowed wavelengths in the Rindler zone (as this only focuses on the unshared wavelength contribution to the energy delta.) Hence, this is simply a first illustration of the energy profile in a case where the seeing zone confinement is applied.

9 Appendix B

Below is the simplified skin depth equation for good conductors.

$$\delta = \sqrt{\frac{2\rho}{2\pi f \mu_r \mu_0}} \tag{24}$$

ρ = resistivity of the conductor
f = frequency of current
μ_r = relative magnetic permeability of the conductor
μ_0 = the permeability of free space

References

[1] A. Froebel. Cable shielding to minimize electromagnetic interference. *EEEIC*.

[2] D. Go and D. A. Pohlman. A mathematical model of the modified paschen's curve for breakdown in microscale gaps. 107:103303 – 103303, 06 2010.

[3] S. Harjo. Partial discharge in high voltage insulating materials. 8:147–163, 03 2016.

[4] S. W. Hawking. Evaporation of two-dimensional black holes. *Phys. Rev. Lett.*, 69:406–409, Jul 1992.

[5] Y. Lau and Y. Liu. From fowler-nordheim relation to the child-langmuir law. 1994.

[6] M. Mcculloch. Inertia from an asymmetric casimir effect. 101, 02 2013.

[7] M. Mcculloch. Low-acceleration dwarf galaxies as tests of quantised inertia. 362, 03 2017.

[8] M. E. McCulloch. Minimum accelerations from quantised inertia. *EPL (Europhysics Letters)*, 90(2):29001, 2010.

[9] E. L. Murphy and R. H. Good. Thermionic emission, field emission, and the transition region. *Phys. Rev.*, 102:1464–1473, Jun 1956.

[10] M. Tajmar. Biefeld-brown effect: Misinterpretation of corona wind phenomena. *AIAA Journal*, 42(2):315–318, Feb 2004.

[11] R. L. Talley. Twenty First Century Propulsion Concept. Technical Report F04611-89-C-0023, VERITAY TECHNOLOGY INC, May 1991.

[12] W. Unruh. Acceleration radiation for orbiting electrons. 307:163–171, 04 1998.

[13] W. G. Unruh. Notes on black-hole evaporation. *Phys. Rev. D*, 14:870–892, Aug 1976.

[14] H. G. White. Q thrusters. In *Pilot Wave Model for Impulsive Thrust from RF Test Device*, Breakthrough Discuss - Day Two, 2018.